

## Construction of a high-affinity receptor site for dihydropyridine agonists and antagonists by single amino acid substitutions in a non-L-type $\text{Ca}^{2+}$ channel

GREGORY H. HOCKERMAN, BLAISE Z. PETERSON, ELIZABETH SHARP, TIMOTHY N. TANADA, TODD SCHEUER, AND WILLIAM A. CATTERALL

Department of Pharmacology, Box 357280, University of Washington, Seattle, WA 98195-7280

Contributed by William A. Catterall, October 27, 1997

**ABSTRACT** The activity of L-type  $\text{Ca}^{2+}$  channels is increased by dihydropyridine (DHP) agonists and inhibited by DHP antagonists, which are widely used in the therapy of cardiovascular disease. These drugs bind to the pore-forming  $\alpha_1$  subunits of L-type  $\text{Ca}^{2+}$  channels. To define the minimal requirements for DHP binding and action, we constructed a high-affinity DHP receptor site by substituting a total of nine amino acid residues from DHP-sensitive L-type  $\alpha_1$  subunits into the S5 and S6 transmembrane segments of domain III and the S6 transmembrane segment of domain IV of the DHP-insensitive P/Q-type  $\alpha_{1A}$  subunit. The resulting chimeric  $\alpha_{1A}/\text{DHPS}$  subunit bound DHP antagonists with high affinity in radioligand binding assays and was inhibited by DHP antagonists with high affinity in voltage clamp experiments. Substitution of these nine amino acid residues yielded 86% of the binding energy of the L-type  $\alpha_{1C}$  subunit and 92% of the binding energy of the L-type  $\alpha_{1S}$  subunit for the high-affinity DHP antagonist PN200–110. The activity of chimeric  $\text{Ca}^{2+}$  channels containing  $\alpha_{1A}/\text{DHPS}$  was increased  $3.5 \pm 0.7$ -fold by the DHP agonist (–)Bay K8644. The effect of this agonist was stereoselective as in L-type  $\text{Ca}^{2+}$  channels since (+) Bay K8644 inhibited the activity of  $\alpha_{1A}/\text{DHPS}$ . The results show conclusively that DHP agonists and antagonists bind to a single receptor site at which they have opposite effects on  $\text{Ca}^{2+}$  channel activity. This site contains essential components from both domains III and IV, consistent with a domain interface model for binding and allosteric modulation of  $\text{Ca}^{2+}$  channel activity by DHPs.

Voltage-gated  $\text{Ca}^{2+}$  channels mediate  $\text{Ca}^{2+}$  influx in response to membrane depolarization and thereby initiate cellular activities such as secretion, contraction, and gene expression. Several types of voltage-gated  $\text{Ca}^{2+}$  channels have been distinguished by their physiological and pharmacological properties and have been designated L, N, P/Q, R, and T (reviewed in refs. 1 and 2). L-Type  $\text{Ca}^{2+}$  channels are the molecular targets for the dihydropyridine (DHP)  $\text{Ca}^{2+}$  channel blockers that are widely used in the therapy of cardiovascular diseases; DHP modulation is the hallmark used to characterize these channels (reviewed in refs. 3 and 4).

The L-type  $\text{Ca}^{2+}$  channels consist of pore-forming  $\alpha_1$  subunits of 190 to 250 kDa in association with disulfide-linked  $\alpha_2\delta$  subunits of approximately 140 kDa, intracellular  $\beta$  subunits of 55 to 72 kDa, and, for the skeletal muscle L-type channel, an additional transmembrane  $\gamma$  subunit of 33 kDa (5). The  $\alpha_1$  subunits confer the characteristic pharmacologic and functional properties of  $\text{Ca}^{2+}$  channels, but their function is modulated by association with the auxiliary subunits. The

pore-forming  $\alpha_1$  subunits can be divided into two distinct families, L-type and non-L-type, that share less than 40% amino acid identity. The L-type  $\alpha_1$  subunit family includes  $\alpha_{1S}$ , which is expressed in skeletal muscle (6),  $\alpha_{1C}$ , which is expressed in cardiac and smooth muscle, neurons, and many other cell types (7–9), and  $\alpha_{1D}$ , which is expressed in endocrine and neuronal cells (10, 11). The non-L-type  $\alpha_1$  subunit family consists of at least three distinct gene products that are expressed primarily in neurons:  $\alpha_{1B}$  (N-type; refs. 12 and 13),  $\alpha_{1A}$  (P/Q-type; refs. 14 and 15), and  $\alpha_{1E}$  (R-type; ref. 16). The  $\alpha_1$  subunits contain four homologous domains (I through IV) that each contain six transmembrane segments (S1 through S6) (6–16).

The DHPs are allosteric modulators that act on L-type  $\text{Ca}^{2+}$  channels as either agonists or antagonists (reviewed in refs. 3, 4, and 17). Charged DHPs are thought to traverse an extracellular pathway to gain access to the DHP receptor site located within the lipid bilayer 11–14 Å from the extracellular surface of the cell membrane (18–21). Photoreactive DHPs specifically label the  $\alpha_1$  subunit of the  $\text{Ca}^{2+}$  channel (5, 22–27). The predominant sites of labeling correspond to transmembrane segment S6 in domain III (IIS6) and transmembrane segment S6 in domain IV (IVS6; refs. 28–31). Analysis of chimeric  $\text{Ca}^{2+}$  channels implicated transmembrane segments IIS5, IIS6, and IVS6 (32–34) in DHP binding. Site-directed mutagenesis of single amino acid residues in segments IIS6 and IVS6 that are conserved in all  $\text{Ca}^{2+}$  channel subtypes had large effects on DHP affinity (35, 36). In addition, mutations of residues that differ between L-type and non-L-type  $\text{Ca}^{2+}$  channels revealed multiple amino acids in transmembrane segments IIS5, IIS6, and IVS6 that are important determinants of high-affinity binding of DHP agonists and antagonists to L-type  $\text{Ca}^{2+}$  channels (34–38). In the experiments reported here, we have substituted nine key amino acid residues that are present in all L-type  $\alpha_1$  subunits into the non-L-type  $\alpha_{1A}$  subunit and measured both activation by DHP agonists and inhibition by DHP antagonists. The results show that these nine amino acid residues are sufficient to constitute a high-affinity receptor site for DHPs that responds appropriately to both DHP agonists and antagonists and is stereoselective like the native DHP receptor of L-type  $\text{Ca}^{2+}$  channels.

### EXPERIMENTAL PROCEDURES

**Construction of Mutant  $\text{Ca}^{2+}$  Channels.** For the construction of  $\alpha_{1A}/\text{DHPS}$ , the *AscI*–*BsrGI* fragment (nucleotides 2582–5408) from  $\alpha_{1A}$  (14) was ligated into pNEB193 (New England Biolabs) and used as template for mutagenic PCR reactions. The mutations in transmembrane segment IIS5 were made in a single PCR reaction using primers that overlapped the *BstXI* (nucleotide 2950) and *ApoI* (nucleotide 4057) sites. The mutagenic mismatches were incorporated by the primer overlapping the *ApoI* site. The mutations in IIS6 were made in a

The publication costs of this article were defrayed in part by page charge payment. This article must therefore be hereby marked “advertisement” in accordance with 18 U.S.C. §1734 solely to indicate this fact.

© 1997 by The National Academy of Sciences 0027-8424/97/9414906-6\$2.00/0  
PNAS is available online at <http://www.pnas.org>.

Abbreviation: DHP, dihydropyridine.

single PCR reaction using primers that overlapped the *XcmI* (nucleotide 4316) and *BspEI* (nucleotide 5102) sites. The mutagenic mismatches were incorporated by the primer overlapping the *XcmI* site. The mutations in IVS6 were made using the splice overlap extension method (39). In the first reactions, mutagenic primers annealing within the cDNA encoding IVS6 were paired with primers that overlapped either the *BspEI* or the *NotI* (nucleotides 5102 and 5384, respectively) sites that flank IVS6. These overlapping fragments were coupled and amplified in a subsequent PCR reaction to give the full-length *BspEI-NotI* fragment containing the mutations in IVS6. The PCR products containing the desired mutations were assembled in *AscI-BsrGI*/pNEB193, and the *AscI-BsrGI* fragment was ligated into full-length  $\alpha_{1A}$  in the expression vector pMT2. The desired mutations were verified, and the integrity of the clone was confirmed by cDNA sequencing and extensive restriction digest analysis.

**Expression of  $Ca^{2+}$  Channels.** Human tsA-201 cells, a simian virus 40 (SV40) T-antigen expressing derivative of the human embryonic kidney cell line HEK293 (a gift of Robert DuBridge, Cell Genesis, Foster City, CA), were maintained in DMEM/F-12 (GIBCO/BRL) enriched with 10% fetal bovine serum. Human tsA-201 cells were cotransfected with  $\alpha_{1A}$ ,  $\alpha_{1A/DHPS}$ , or  $\alpha_{1CH}$  (9);  $\beta_{1b}$  (40);  $\alpha_{2\delta}$  (41); and CD8 antigen (EBO-pCD-Leu2, American Type Culture Collection) such that the molar ratio of the plasmids was 1:1:1:0.8. Cells were transfected by  $Ca^{2+}$  phosphate precipitation (42), and cells were replated at low density for electrophysiological recording 20–24 hours later. The  $\alpha_{1CH}$  cDNA was in the expression plasmid ZEM 229 (a gift of Eileen Mulvihill, Zymogenetics, Seattle). The  $\alpha_{2\delta}$  cDNA was in the expression plasmid ZEM 228 (a gift of Eileen Mulvihill). The  $\alpha_{1A}$ ,  $\alpha_{1A/DHPS}$ , and  $\beta_{1b}$  cDNA were in the expression plasmid pMT2 (Genetics Institute, Boston).

**Electrophysiology.** Transfectants were recognized by labeling with anti-CD8 antibody-coated beads (M450 CD8 Dynabeads, Dynal). Barium currents through  $Ca^{2+}$  channels were recorded using the whole-cell configuration of the patch clamp technique. Patch electrodes were pulled from VWR micropipettes and fire-polished to produce an inner tip diameter of 4–6  $\mu\text{m}$ . Currents were recorded using an Axon Instruments Axopatch 200B patch clamp amplifier and filtered at 1 or 2 kHz (8-pole Bessel filter, -3 dB). Voltage pulses were applied and data were acquired using pClamp6 software (Axon Instruments). Linear leak and capacitance currents have been subtracted using an on-line P/-4 subtraction paradigm. ( $\pm$ )PN200-110 was applied to cells using a fast perfusion system with background perfusion. (-)Bay K 8644 was added to the bath, without background perfusion, as a 10 $\times$  stock. The bath saline contained 150 mM of Tris, 2 mM of  $MgCl_2$ , and 10 mM of  $BaCl_2$ . The intracellular saline contained 130 mM of *N*-methyl-D-glucamine, 10 mM of EGTA, 60 mM of HEPES, 2 mM of  $MgATP$ , and 1 mM of  $MgCl_2$ . The pH of both solutions was adjusted to 7.3 with methanesulfonic acid. All experiments were performed at room temperature (20–23°C).

**Preparation of Membranes.** Transfected tsA-201 cells were washed twice, scraped from the cell culture dish, and homogenized using a glass-teflon homogenizer in Buffer A (50 mM of Tris/100  $\mu\text{M}$  of phenylmethylsulfonyl fluoride/100  $\mu\text{M}$  of benzamidine/1.0  $\mu\text{M}$  of pepstatin A/1.0  $\mu\text{g/ml}$  of leupeptin/2.0  $\mu\text{g/ml}$  of aprotinin, pH 8.0). The homogenate was centrifuged at 700  $\times g$  for 5 min. The resulting pellet was discarded and the supernatant was centrifuged 30 min at 100,000  $\times g$ . The supernatant was discarded and the membrane pellet was washed and homogenized in Buffer A. The resulting membrane homogenate was divided into aliquots and stored at -80°C for up to 3 months with no detectable loss of (+)- $[^3H]$ PN200-110 binding activity.

**Radioligand Binding.** Equilibrium binding assays were performed in Buffer A with 20–200  $\mu\text{g}$  of membrane protein,

0.01–5 nM of (+)- $[^3H]$ PN200-110, and 1 mM of  $Ca^{2+}$  at 32°C for 180–210 min. Nonspecific binding was determined in the presence of 1  $\mu\text{M}$  ( $\pm$ )-PN200-110, and bound and free ligands were separated by vacuum filtration over GF/C glass fiber filters. Filters were washed using ice-cold wash buffer (10 mM of Tris/1% polyethylene glycol 8000/0.1% BSA/0.01% Triton X-100, pH 8.0), and bound radioactivity was detected by liquid scintillation counting. Dissociation constants ( $K_D$ ) were determined using the radioligand data analysis program LIGAND (Biosoft, Cambridge, U.K.). All data are means  $\pm$  SEM.

## RESULTS

**Construction of a High Affinity DHP Site in  $\alpha_{1A}$ .** The key amino acid residues required for high affinity DHP binding as determined in previous studies are illustrated in Fig. 1. Photoaffinity labeling followed by antibody mapping of the labeled peptide fragments showed that transmembrane segments IIIS6 and IVS6 are components of the DHP receptor site in L-type  $Ca^{2+}$  channels (refs. 28 and 29; Fig. 1A, shaded segments). Construction and analysis of chimeric  $Ca^{2+}$  channels confirmed the importance of transmembrane segments IIIS6 (32) and IVS6 (32–34) and further demonstrated an important role of transmembrane segment IIIS5 (ref. 32; Fig. 1A, diagonally hatched segment). Mutation of single amino acid residues identified three conserved amino acid residues in transmem-

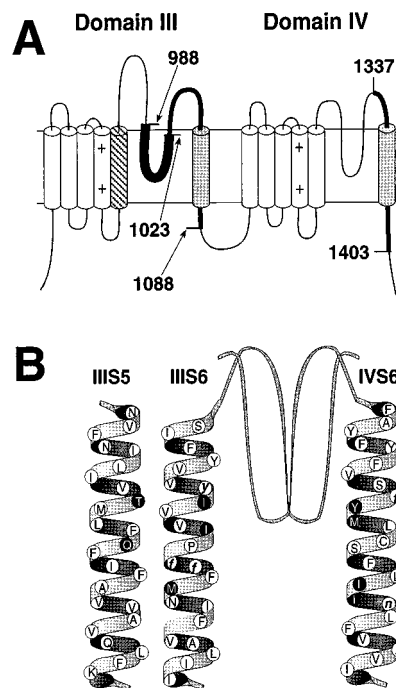


**FIG. 1.** Localization of the DHP binding site in L-type channels. (A) Studies utilizing DHP photoaffinity labels and site-directed antibodies (28, 29) identified transmembrane segments IIIS6 and IVS6 of L-type  $Ca^{2+}$  channels as components of the DHP binding site. Boundaries of the labeled peptides (shaded cylinders and thick lines) are shown as amino acid sequence numbers from  $\alpha_{1S}$  (6). Subsequent studies utilizing chimeric  $Ca^{2+}$  channels further demonstrated the role of IIIS6 and IVS6 as well as transmembrane domain IIIS5 in DHP modulation of L-type channels (32–34). (B) Structure of  $\alpha_{1A/DHPS}$ . Studies of single amino acid substitutions in L-type channels revealed nine L-type-specific (black circles with white letters) and five conserved (white circles with black lower case letters) amino acid residues to be critical for DHP binding and block of L-type channels (34–38). The nine L-type-specific amino acid residues critical for DHP action were inserted into the DHP-insensitive  $\alpha_{1A}$  subunit amino acid sequence (14) (white circles with black letters) to construct a mutant  $\alpha_{1A}$  subunit that is modulated by DHPs ( $\alpha_{1A/DHPS}$ ).

brane segment IIIS6 and two in IVS6 that are important for DHP binding and are present in all  $\text{Ca}^{2+}$  channels (refs. 35 and 36; Fig. 1B, white circles, lowercase letters). In addition, two L-type-specific residues in segment IIIS5, three in segment IIIS6, and four in segment IVS6 were found to be important for DHP binding (refs. 34–38; Fig. 1B, dark circles). The success of experiments with chimeric  $\text{Ca}^{2+}$  channels in which segments of L-type  $\text{Ca}^{2+}$  channels are transferred into non-L-type  $\text{Ca}^{2+}$  channels suggests that the basic structure of non-L-type channels is appropriate to support DHP binding, even though the amino acid sequence is less than 40% identical. Similarly, the requirement for amino acid residues that are conserved between L-type and non-L-type  $\text{Ca}^{2+}$  channels for high-affinity DHP binding suggests that the DHP binding site contains structural features that are common to all  $\text{Ca}^{2+}$  channels. If all of the L-type-specific amino acid residues that are required for high affinity DHP binding have been identified, substitution of the nine amino acid residues highlighted as dark circles in Fig. 1B into a non-L-type  $\text{Ca}^{2+}$  channel should be sufficient to construct a high-affinity DHP binding site. To test this idea, we substituted these nine amino acid residues for their counterparts in the DHP-insensitive rBa isoform of the  $\alpha_{1A}$  subunit of P/Q-type  $\text{Ca}^{2+}$  channels using site-directed mutagenesis methods as described in *Experimental Procedures*.

**Functional Characteristics of the DHP-Sensitive  $\alpha_{1A}$  Chimera.** The resulting  $\alpha_{1A}/\text{DHPS}$  subunit was expressed in tsA-201 cells with  $\alpha_{2\delta}$  and  $\beta_{1b}$  subunits and analyzed by whole cell voltage clamp as described in *Experimental Procedures*. Barium currents through the  $\alpha_{1A}/\text{DHPS}$  subunit activated normally but inactivated more rapidly than wild-type  $\alpha_{1A}$  (Fig. 2A;  $\alpha_{1A}$ ,  $\tau_h = 279$  ms;  $\alpha_{1A}/\text{DHPS}$ ,  $\tau_h = 123$  ms). The two channels had similar current-voltage relationships with peak barium current near 0 mV (Fig. 2B). However, the voltage dependence of inactivation of  $\alpha_{1A}/\text{DHPS}$  was shifted 40 mV toward more negative membrane potentials compared with wild-type  $\alpha_{1A}$  (Fig. 2C;  $\alpha_{1A}$ ,  $V_{h/2} = -48$  mV;  $\alpha_{1A}/\text{DHPS}$ ,  $V_{h/2} = -88$  mV). Thus, the  $\alpha_{1A}/\text{DHPS}$  chimera is functional as a  $\text{Ca}^{2+}$  channel, but has altered inactivation properties.

**Inhibition of Barium Currents Through  $\alpha_{1A}/\text{DHPS}$  by a DHP Antagonist.** DHP antagonists bind with higher affinity to the inactivated state of L-type  $\text{Ca}^{2+}$  channels (43–45). To compare the DHP sensitivity of wild-type  $\alpha_{1A}$  and  $\alpha_{1A}/\text{DHPS}$ , we compensated for the shift in the voltage dependence of inactivation by measuring the block of barium currents from holding potentials that differed by 40 mV:  $-80$  mV for  $\alpha_{1A}$  and  $-120$  mV for  $\alpha_{1A}/\text{DHPS}$ . These conditions yield the same ratio of resting and inactivated channels for each  $\alpha_1$  subunit. The more negative membrane potential used for the  $\alpha_{1A}/\text{DHPS}$  chimera would reduce inhibition of L-type  $\text{Ca}^{2+}$  channels by DHPs, so it is unlikely that this membrane potential per se would increase inhibition of the  $\alpha_{1A}/\text{DHPS}$  chimera.

The high-affinity DHP antagonist PN200–110 (isradipine) had no effect on P/Q-type  $\text{Ca}^{2+}$  channels containing  $\alpha_{1A}$ , even at the high concentration of  $10 \mu\text{M}$  (Fig. 3A). In contrast, chimeric  $\text{Ca}^{2+}$  channels containing  $\alpha_{1A}/\text{DHPS}$  were substantially inhibited by  $10$  nM of PN200–110 and completely inhibited by  $100$  nM of PN200–110 (Fig. 3A). The  $\text{IC}_{50}$  value estimated from titration experiments was  $13.8 \text{ nM} \pm 3 \text{ nM}$  (Fig. 3C,  $n = 9$ ). This compares favorably with the  $\text{IC}_{50}$  of  $6.8 \text{ nM} \pm 1 \text{ nM}$  for block of L-type  $\text{Ca}^{2+}$  channels containing  $\alpha_{1C}$  expressed with  $\alpha_{2\delta}$  and  $\beta_{1b}$  in the same cell line (Fig. 3B).  $\text{Ca}^{2+}$  channels containing  $\alpha_{1A}$  are unaffected by PN200–110 up to at least  $10 \mu\text{M}$ . Based on this, the minimum estimate of the  $\text{IC}_{50}$  for inhibition of P/Q-type  $\text{Ca}^{2+}$  channels containing  $\alpha_{1A}$  is  $250 \mu\text{M}$ , more than four orders of magnitude higher than for  $\alpha_{1A}/\text{DHPS}$ . Thus, substitution of nine amino acid residues in  $\alpha_{1A}$  is sufficient to constitute a high affinity receptor site for a DHP antagonist with more than 10,000-fold higher affinity than wild-type  $\alpha_{1A}$ .

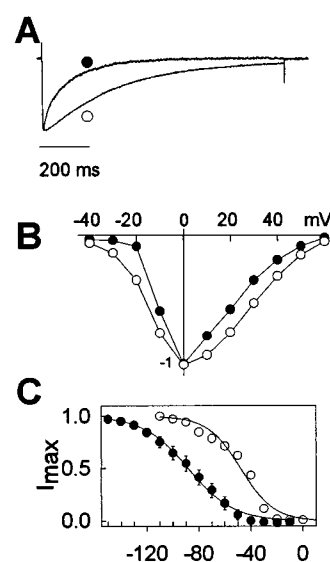


FIG. 2. Biophysical properties of  $\text{Ca}^{2+}$  channels containing  $\alpha_{1A}$  and  $\alpha_{1A}/\text{DHPS}$ . (A)  $\text{Ca}^{2+}$  currents were evoked from cells expressing  $\alpha_{1A}$  (open circle) or  $\alpha_{1A}/\text{DHPS}$  (solid circle) subunits along with the  $\beta_{1b}$  and  $\alpha_{2\delta}$  subunits by a 1 s depolarization to 0 mV from a holding potential of  $-120$  mV ( $\alpha_{1A}/\text{DHPS}$ ) or  $-80$  mV ( $\alpha_{1A}$ ). Current amplitudes were normalized to facilitate comparison of inactivation kinetics. The time courses of inactivation were fit to a single exponential function. The time constant of inactivation ( $\tau$ ) was  $279 \pm 28$  ms ( $n = 6$ ) for wild type and  $123 \pm 6$  ms ( $n = 6$ ) for the mutant. (B) Current-voltage relationships for  $\text{Ca}^{2+}$  channels containing  $\alpha_{1A}$  or  $\alpha_{1A}/\text{DHPS}$ . From a holding potential of  $-120$  mV ( $\alpha_{1A}/\text{DHPS}$ ; solid circles) or  $-80$  mV ( $\alpha_{1A}$ , open circles), the membrane potential was depolarized in 10 mV increments for 100 ms to test pulse potentials from  $-40$  mV to  $+60$  mV and barium currents were recorded. (C) Voltage-dependent inactivation of  $\text{Ca}^{2+}$  channels containing  $\alpha_{1A}$  (open circles) and  $\alpha_{1A}/\text{DHPS}$  (solid circles). Cells expressing  $\alpha_{1A}$  or  $\alpha_{1A}/\text{DHPS}$  were held at  $-80$  mV or  $-120$  mV, respectively. From these holding potentials, cells were depolarized to the indicated conditioning pulse potentials for 10 seconds, followed immediately by a 100 ms test pulse to 0 mV. The amplitude of the  $\text{Ca}^{2+}$  current during the test pulse is plotted against the voltage of the preceding 10 s conditioning pulse. Smooth lines are fits to a Boltzman function with slope factors of 12.7 and 17.3 for  $\alpha_{1A}$  and  $\alpha_{1A}/\text{DHPS}$ , respectively. For  $\alpha_{1A}$ ,  $V_{h/2} = -47.7 \pm 1.8$  mV ( $n = 6$ ), and for  $\alpha_{1A}/\text{DHPS}$ ,  $V_{h/2} = -88.1 \pm 1.0$  mV ( $n = 4$ ).

**Increase of Barium Currents Through  $\alpha_{1A}/\text{DHPS}$  by a DHP Agonist.** DHPs are allosteric modulators of L-type  $\text{Ca}^{2+}$  channels and can either inhibit or enhance channel activity (3, 4, 17). Activation of L-type  $\text{Ca}^{2+}$  channels is increased by DHP agonists like  $(-)$ Bay K8644 (17). Our previous results on mutations in the  $\alpha_{1S}$  subunit of L-type  $\text{Ca}^{2+}$  channels indicated that many of the same amino acid residues are required for binding of both DHP agonists and antagonists (35). To test whether DHP agonists can also bind and act at the minimal DHP receptor site constructed in  $\alpha_{1A}/\text{DHPS}$ , we measured barium currents from a holding potential of  $-100$  mV in the presence and absence of  $10 \mu\text{M}$   $(-)$  Bay K8644 (Fig. 4). Bay K8644 increased  $\text{Ca}^{2+}$  currents through L-type  $\text{Ca}^{2+}$  channels containing  $\alpha_{1C}$ , but had no effect on P/Q-type channels containing  $\alpha_{1A}$  (Fig. 4 Left). In contrast,  $(-)$  Bay K8644 increased barium currents through chimeric  $\text{Ca}^{2+}$  channels containing  $\alpha_{1A}/\text{DHPS}$  by  $3.53 \pm 0.66$ -fold (Fig. 4 Left;  $n = 3$ ). The increased barium current was observed over a wide range of test pulse potentials, as for L-type  $\text{Ca}^{2+}$  channels containing  $\alpha_{1C}$  (Fig. 4 Right). In contrast,  $(-)$  Bay K8644 had no effect on barium currents through P/Q-type  $\text{Ca}^{2+}$  channels containing  $\alpha_{1A}$  at any test pulse potential (Fig. 4 Right). Thus, the minimal DHP receptor site of  $\alpha_{1A}/\text{DHPS}$  is sufficient for both binding and functional effect of a DHP agonist.



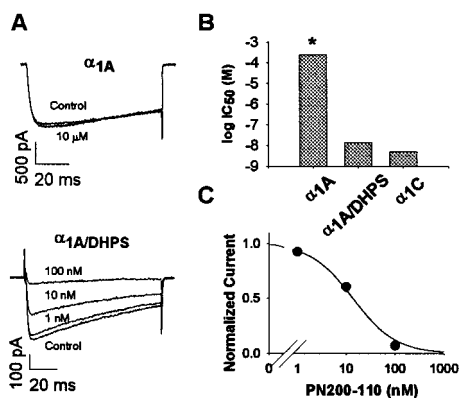


FIG. 3. Inhibition of  $\text{Ca}^{2+}$  channels containing  $\alpha_{1A}$ ,  $\alpha_{1C}$ , and  $\alpha_{1A/DHPS}$  subunits by the DHP antagonist PN200-110. (A) Representative current traces from cells expressing  $\alpha_{1A}$  or  $\alpha_{1A/DHPS}$  in the presence and absence of the indicated concentrations of PN200-110. Cells expressing  $\alpha_{1A}$  or  $\alpha_{1A/DHPS}$  were held at  $-80$  or  $-120$ , respectively, and depolarized to  $0$  mV for  $100$  ms every  $20$  seconds. After a control baseline had been established, PN200-110 was perfused onto the cells at the concentrations indicated. (B)  $\text{IC}_{50}$  values for inhibition of  $\alpha_{1A}$ ,  $\alpha_{1A/DHPS}$ , and  $\alpha_{1C}$  by PN200-110. The  $\text{IC}_{50}$  for the  $\alpha_{1A/DHPS}$  channel was  $13.8 \pm 3.0$  nM ( $n = 9$ ); for the  $\alpha_{1C}$  channel,  $\text{IC}_{50}$  was  $6.8 \pm 1.2$  nM (36). The asterisk over the  $\text{IC}_{50}$  value for the  $\alpha_{1A}$  channel ( $250$   $\mu\text{M}$ ) is to indicate that this value is a lower limit since no block was detected at  $10$   $\mu\text{M}$  PN200-110, the highest concentration studied. (C) Concentration-response curve of  $\alpha_{1A/DHPS}$  for PN200-110. The mean data were fit to the equation  $1 - 1/(1 + ([\text{IC}_{50}]/[\text{PN200-110}]))$ . Standard error ( $n = 9$ ) was smaller than the diameter of the symbols in the figure. Current amplitudes at each drug concentration were expressed as a fraction of the current amplitude in the absence of drug.

The functional effects of many DHP agonists are stereospecific. For Bay K8644, the (–) enantiomer is an agonist while the (+) isomer is an antagonist (17). As for L-type  $\text{Ca}^{2+}$  channels containing  $\alpha_{1C}$ , we found that chimeric  $\text{Ca}^{2+}$  channels containing  $\alpha_{1A/DHPS}$  are inhibited by (+) Bay K8644 ( $\text{IC}_{50} = 303 \pm 102$  nM,  $n = 8$ ; data not shown), and no activating effect of (+) Bay K8644 was observed at any concentration tested. Thus, the stereoselectivity of DHP binding and action is also present in the minimal DHP receptor site constructed in  $\alpha_{1A/DHPS}$ .

**High Affinity Binding of PN200-110 to  $\alpha_{1A/DHPS}$  in Cell Membrane Preparations.** Inhibition of barium currents by PN200-110 measures primarily drug binding to the resting state of  $\text{Ca}^{2+}$  channels that is predominant at the negative holding potential. Because DHP antagonists have higher affinity for the inactivated state of  $\text{Ca}^{2+}$  channels (43–45), their binding affinity is higher in radioligand binding assays using membrane preparations whose membrane potential is near  $0$  mV where inactivation is complete. We first compared binding of [ $^3\text{H}$ ]PN200-110 at a fixed concentration of  $4.4$  nM.  $\text{Ca}^{2+}$  channels containing  $\alpha_{1C}$  bound [ $^3\text{H}$ ]PN200-110 specifically ( $63.7$  fmol/mg cell protein) while those containing  $\alpha_{1A}$  did not have significant specific binding. As expected from the electrophysiological results,  $\text{Ca}^{2+}$  channels containing  $\alpha_{1A/DHPS}$  also bound [ $^3\text{H}$ ]PN200-110 specifically ( $36.9$  fmol/mg cell protein), but not as well as channels containing  $\alpha_{1C}$ . To compare the binding affinity of  $\alpha_{1C}$  and  $\alpha_{1A/DHPS}$  quantitatively, we carried out a saturation binding study (Fig. 5A) and analyzed the data by Scatchard plot (Fig. 5B, note the different axes for  $\alpha_{1C}$  and  $\alpha_{1A/DHPS}$ ). The results indicate a  $K_D$  for binding to  $\alpha_{1C}$  of  $50$  pM compared with a  $K_D$  for  $\alpha_{1A/DHPS}$  of  $1.48$  nM, 27-fold higher. Thus, the  $\alpha_{1A/DHPS}$  chimera has high affinity for PN200-110 in a radioligand binding assay as well as in electrophysiological experiments, but the difference in binding between  $\alpha_{1C}$  and  $\alpha_{1A/DHPS}$  is greater in the ligand binding assay.

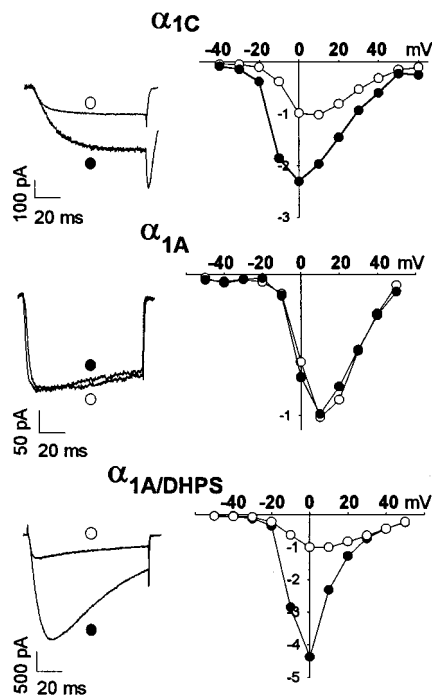


FIG. 4. Modulation of  $\text{Ca}^{2+}$  channels containing  $\alpha_{1C}$ ,  $\alpha_{1A}$ , or  $\alpha_{1A/DHPS}$  subunits by the DHP agonist (–) Bay K8644. (Left) Current traces from cells expressing the indicated channel types in the absence and presence of  $10$   $\mu\text{M}$  of (–) Bay K8644. Cells expressing  $\alpha_{1A}$ , or  $\alpha_{1A/DHPS}$  were depolarized from a holding potential of  $-100$  mV to  $0$  mV for  $100$  ms. Cells expressing  $\alpha_{1C}$  were held at  $-60$  mV and depolarized to  $+10$  mV for  $100$  ms. For  $\text{Ca}^{2+}$  channels containing  $\alpha_{1A}$  or  $\alpha_{1A/DHPS}$ , a series of ten  $1$  s depolarizations to  $0$  mV was used to bring the agonist effect to equilibrium. (Right) Current-voltage relationship before and after addition of  $10$   $\mu\text{M}$  of (–) Bay K8644 is shown for each channel type. The peak current amplitude of each I/V curve in the absence of (–) Bay K8644 was set to 1, and the current amplitudes in the presence of (–) Bay K8644 were expressed relative to the current amplitudes in the absence of drug. Cells expressing  $\alpha_{1A}$  or  $\alpha_{1A/DHPS}$  were held at  $-80$  mV or  $-120$  mV, respectively. From these holding potentials, cells were depolarized to the indicated test pulse potentials from  $-50$  mV to  $+50$  mV in  $10$  mV increments for  $100$  ms, and barium currents were recorded.

## DISCUSSION

**Molecular Requirements for a High Affinity DHP Receptor Site.** Substitution of nine amino acid residues previously shown to be required for DHP binding (34–38) into the sequence of the non-L-type  $\alpha_{1A}$  subunit is sufficient to construct a high-affinity DHP receptor site. This site was constructed in the structural context of the  $\alpha_{1A}$  subunit that contains at least five conserved residues that are necessary for high-affinity DHP binding (35, 36). The resulting chimera  $\alpha_{1A/DHPS}$  has many of the pharmacological properties of an L-type  $\text{Ca}^{2+}$  channel with respect to DHPs. The  $\text{IC}_{50}$  for inhibition of  $\text{Ca}^{2+}$  current by PN200-110 is  $13.8$  nM, only twofold higher than the  $\text{IC}_{50}$  value for inhibition of L-type  $\text{Ca}^{2+}$  channels containing  $\alpha_{1C}$  expressed under the same conditions. Inhibition of barium currents measures primarily the affinity of the resting state for DHPs because of the negative holding potential used in these experiments. In contrast, the binding experiments on membranes from transfected cells measure primarily the higher affinity of the inactivated state because of the prolonged depolarization of the membranes in the binding assay. The  $K_D$  for binding of [ $^3\text{H}$ ]PN200-110 to  $\text{Ca}^{2+}$  channels containing  $\alpha_{1A/DHPS}$  is  $1.48$  nM, compared with  $55$  pM for L-type  $\text{Ca}^{2+}$  channels containing  $\alpha_{1C}$  (36) and  $250$  pM L-type  $\text{Ca}^{2+}$  channels containing  $\alpha_{1S}$  (35) expressed under the same conditions. Thus, the amino acid substitutions in  $\alpha_{1A/DHPS}$  are more

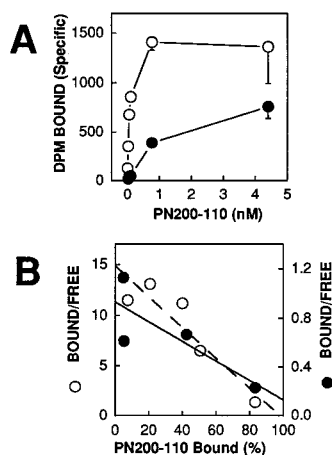


FIG. 5. Binding of [ $^3$ H]PN200-110 to membrane preparations from cells expressing  $\alpha_{1C}$  or  $\alpha_{1A/DHPS}$  channels. (A) Equilibrium binding of [ $^3$ H]PN200-110 to membrane preparations from cells expressing  $\alpha_{1C}$  (open circles) or  $\alpha_{1A/DHPR}$  (solid circles) subunits. Specific binding was determined by subtracting nonspecific binding of [ $^3$ H]PN200-110 in the presence of 1  $\mu$ M of unlabeled PN200-110 from total binding in the absence of the unlabeled drug at each [ $^3$ H]PN200-110 concentration. Means of the data at each concentration are plotted  $\pm$  SEM ( $n = 3$ ). (B) Scatchard analysis of equilibrium binding of [ $^3$ H]PN200-110 to  $\alpha_{1C}$  (open circles; dashed line) and  $\alpha_{1A/DHPS}$  channels (solid circles; solid line). The ordinate axes are different for each subunit type to normalize the data. The  $K_D$  values in this experiment were 79 pM for  $\alpha_{1C}$  and 1.48 nM for  $\alpha_{1A/DHPS}$ .

effective in establishing binding and block of resting  $Ca^{2+}$  channels than inactivated  $Ca^{2+}$  channels. Nevertheless, of the  $-14.3$  kcal/mol and  $-13.4$  kcal/mol binding energy calculated from the  $K_D$  values for PN200-110 binding to  $\alpha_{1C}$  and  $\alpha_{1S}$ , respectively,  $-12.3$  kcal/mol (86% of  $\alpha_{1C}$  or 92% of  $\alpha_{1S}$ ) is observed in  $\alpha_{1A/DHPS}$ . The remaining binding energy of  $\alpha_{1C}$  and  $\alpha_{1S}$  may be contributed by several amino acid residues whose mutation had measurable, but less than twofold, effects on DHP binding affinity (35, 36) or by the overall structural context of  $\alpha_{1A}$  versus  $\alpha_{1C}$  and  $\alpha_{1S}$ .

**A Single Receptor Site for DHP Agonists and Antagonists.** DHP agonists inhibit high-affinity binding of DHP antagonists, consistent with the idea that they share the same receptor site (45-47). However, binding studies on intact cells reveal complex interactions between binding of agonist and antagonist DHPs, and it has been hypothesized that agonists and antagonists occupy different sites when causing their opposite effects on  $Ca^{2+}$  channel function (48). In contrast to this hypothesis, our results show conclusively that DHP agonists and antagonists occupy the same receptor site and cause opposite effects on  $Ca^{2+}$  channel activity when bound there. Each of the nine single amino acids substituted in  $\alpha_{1A/DHPS}$  is required for high-affinity antagonist binding in L-type  $Ca^{2+}$  channels, and mutations of many of these residues also reduce affinity for binding of agonists to L-type channels. Construction of a minimal DHP receptor site for high-affinity antagonist binding also is sufficient to confer stereoselective agonist binding and action. Molecular differences in the interactions of these two classes of drugs with the same receptor site must be responsible for the dramatic differences in their pharmacological effects.

**A Domain-Interface Model for DHP Binding and Action.** Based on the original photoaffinity labeling of the DHP receptor site, it was proposed that DHPs bind to a single site at the interface of domains III and IV (30). This model is confirmed by the results presented here, which show that the minimal receptor site sufficient for high-affinity binding of DHP antagonists and for stereoselective binding and action of DHP agonists includes amino acid residues in transmembrane

segments S5 and S6 in domain III and transmembrane S6 in domain IV. Allosteric effectors of enzymes most often bind to sites at the interfaces between subunits or domains (e.g., refs. 49 and 50), and current evidence indicates that the agonist binding site of nicotinic acetylcholine receptors is at a subunit interface (51). Evidently, these sites are particularly sensitive to binding of small ligands, which can alter interactions between domains or subunits when bound at their interface. Based on these analogies, it is likely that DHPs act as allosteric effectors that alter domain-domain interactions within the  $\alpha_1$  subunits of  $Ca^{2+}$  channels. Determination of the structural basis for the opposite, stereoselective effects of DHP agonists and antagonists on  $Ca^{2+}$  channel function when bound at the DHP receptor site between domains III and IV will provide further information on the mechanism of action of these drugs and on the interactions between these  $Ca^{2+}$  channel domains in channel gating.

1. Tsien, R. W., Lipscombe, D., Madison, D., Bley, K. & Fox, A. (1995) *Trends Neurosci.* **18**, 52-54.
2. Dunlap, K., Luebke, J. I. & Turner, T. J. (1995) *Trends Neurosci.* **18**, 89-98.
3. McDonald, T. F., Pelzer, S., Trautwein, W. & Pelzer, D. J. (1994) *Physiol. Rev.* **74**, 365-707.
4. Hockerman, G. H., Peterson, B. Z., Johnson, B. D. & Catterall, W. A. (1997) *Annu. Rev. Pharmacol. Toxicol.* **37**, 361-397.
5. Takahashi, M., Seagar, M. J., Jones, J. F., Reber, B. F. & Catterall, W. A. (1987) *Proc. Natl. Acad. Sci. USA* **84**, 5478-5482.
6. Tanabe, T., Takeshima, H., Mikami, A., Flockerzi, V., Takahashi, H., Kangawa, K., Kojima, M., Matsuo, H., Hirose, T. & Numa, S. (1987) *Nature (London)* **328**, 313-318.
7. Mikami, A., Imoto, K., Tanabe, T., Niidome, T., Mori, Y., Takeshima, H., Narumiya, S. & Numa, S. (1989) *Nature (London)* **340**, 230-233.
8. Koch, W. J., Ellinor, P. T. & Schwartz, A. (1990) *J. Biol. Chem.* **265**, 17786-17791.
9. Snutch, T. P., Tomlinson, W. J., Leonard, J. P. & Gilbert, M. M., (1991) *Neuron* **7**, 45-47.
10. Williams, M. E., Feldman, D. H., McCue, A. F., Brenner, R., Velicelebi, G., Ellis, S. B. & Harpold, M. M. (1992) *Neuron* **8**, 71-84.
11. Seino, S., Chen, L., Seino, M., Blondel, O., Takeda, J., Johnson, J. H. & Bell, G. I. (1992) *Proc. Natl. Acad. Sci. USA* **89**, 584-588.
12. Dubel, S. J., Starr, V. B., Hell, J., Ahljanian, M. K., Eneart, J. J., Catterall, W. A. & Snutch, T. P. (1992) *Proc. Natl. Acad. Sci. USA* **89**, 5058-5062.
13. Williams, M. E., Brust, P. F., Feldman, D. H., Patthi, S., Simerson, S., Maroufi, A., McCue, A. F., Velicelebi, G., Ellis, S. B. & Harpold, M. M. (1992) *Science* **257**, 389-395.
14. Starr, V. B., Prystay, W. & Snutch, T. P. (1991) *Proc. Natl. Acad. Sci. USA* **88**, 5621-5625.
15. Mori, Y., Friedrich, T., Kim, M.-S., Mikami, A., Nakai, J., Ruth, P., Bosse, E., Hofmann, F., Flockerzi, V., Furuichi, T., Mikoshiba, K., Imoto, K., Tanabe, T. & Numa, S. (1991) *Nature (London)* **350**, 398-402.
16. Soong, T. W., Stea, A., Hodson, C. D., Dubel, S. J., Vincent, S. R. & Snutch, T. P. (1993) *Science* **260**, 1133-1136.
17. Bechem, M. & Schramm, M. (1987) *J. Mol. Cell. Cardiol.* **19**, 63-75.
18. Kass, R. S. & Arena, J. P. (1989) *J. Gen. Physiol.* **93**, 1109-1127.
19. Kass, R. S., Arena, J. P. & Chin, S. (1991) *J. Gen. Physiol.* **98**, 63-75.
20. Strubing, C., Hering, S. & Glossman, H. (1993) *Br. J. Pharmacol.* **108**, 884-891.
21. Bangalore, R., Baidur, N., Rutledge, A., Triggle, D. J. & Kass, R. S. (1994) *Mol. Pharmacol.* **46**, 660-666.
22. Ferry, D. R., Rombusch, M., Goll, A. & Glossman, H. (1984) *FEBS Lett.* **169**, 112-167.
23. Galizzi, J. P., Borsotto, M., Barhanin, J., Fosset, M. & Lazdunski, M. (1986) *J. Biol. Chem.* **261**, 1393-1397.
24. Sharp, A. H., Imagawa, T., Leung, A. T. & Campbell, K. P. (1987) *J. Biol. Chem.* **262**, 12309-12315.
25. Vaghy, P. L., Striessnig, J., Miwa, K., Knause, H.-G., Itagaki, K., McKenna, E., Glossmann, H. & Striessnig, J. (1987) *J. Biol. Chem.* **262**, 14337-14342.

26. Sieber, M., Nastainczyk, W., Zubor, V., Werner, W. & Hofmann, F. (1987) *Eur. J. Biochem.* **167**, 117–122.
27. Hosey, M. M., Barhanin, J., Schmid, A., Vandaele, S., Ptasiński, J., O'Callahan, C., Cooper, C. & Lazdunski, M. (1987) *Biochem. Biophys. Res. Commun.* **147**, 1137–1145.
28. Striessnig, J., Murphy, B. J. & Catterall, W. A. (1991) *Proc. Natl. Acad. Sci. USA* **88**, 10769–10773.
29. Nakayama, H., Taki, M., Striessnig, J., Catterall, W. A. & Kanaoka, Y. (1991) *Proc. Natl. Acad. Sci. USA* **88**, 9203–9207.
30. Catterall, W. A. & Striessnig, J. (1992) *Trends Pharmacol. Sci.* **13**, 256–262.
31. Kalasz, H., Watanabe, T., Yabana, H., Itagaki, K., Naito, K., Nakayama, H., Schwartz, A. & Vaghy, P. L. (1993) *FEBS Lett.* **331**, 177–181.
32. Grabner, M., Wang, Z. Y., Hering, S., Striessnig, J. & Glossmann, H. (1996) *Neuron* **16**, 207–218.
33. Tang, S., Yatani, A., Bahinski, A., Mori, Y. & Schwartz, A. (1993) *Neuron* **11**, 1013–1021.
34. Schuster, A., Lacinova, L., Klugbauer, N., Ito, H., Birnbaumer, L. & Hofmann, F. (1996) *EMBO J.* **15**, 2365–2370.
35. Peterson, B. Z., Tanada, T. N. & Catterall, W. A. (1996) *J. Biol. Chem.* **271**, 5293–5296.
36. Peterson, B. Z., Johnson, B. D., Hockerman, G. H., Acheson, M., Scheuer, T. & Catterall, W. A. (1997) *J. Biol. Chem.* **272**, 18752–18758.
37. Mitterdorfer, J., Wang, Z., Sinnegger, M. J., Hering, S., Striessnig, J., Grabner, M. & Glossmann, H. (1996) *J. Biol. Chem.* **271**, 30330–30335.
38. He, M., Bodi, I., Mikala, G. & Schwartz, A. (1997) *J. Biol. Chem.* **272**, 2629–2633.
39. Ho, S. N., Hunt, H. D., Horton, R. M., Pullen, J. K. & Pease, L. R. (1989) *Gene* **77**, 51–59.
40. Pragnell, M., Leveille, C. F., Jay, S. D. & Campbell, K. P. (1991) *FEBS Lett.* **291**, 253–257.
41. Ellis, S. B., Williams, M. E., Ways, N. R., Brenner, R., Sharp, A. H., Leung, A. T., Campbell, K. P., McKenna, E., Koch, W. J., Hui, A., Schwartz, A. & Harpold, M. M. (1988) *Science* **241**, 1661–1664.
42. Margolskee, R. F., McHendry-Rinde, B. & Horne, R. (1994) *Biotechniques* **15**, 906–911.
43. Kokubun, S. & Reuter, H. (1984) *Proc. Natl. Acad. Sci. USA* **81**, 4824–4827.
44. Bean, B. P. (1984) *Proc. Natl. Acad. Sci. USA* **81**, 6388–6392.
45. Sanguinetti, M. & Kass, R. (1984) *Circ. Res.* **55**, 336–348.
46. Janis, R. A., Sarmiento, J. G., Maurer, S. C., Bolger, G. T. & Triggle, D. J. (1984) *J. Pharmacol. Exp. Ther.* **231**, 8–15.
47. Greenberg, D. A., Cooper, E. C. & Carpenter, C. L. (1984) *Brain Res.* **305**, 365–368.
48. Porzig, H., Kokubun, S., Prod'hom, B., Becker, C. & Reuter, H. (1987) *Biochim. Biophys. Acta* **46**, S370–374.
49. Barford, D. & Johnson, L. (1989) *Nature (London)* **340**, 609–616.
50. Kantrowitz, E. & Lipscomb, W. N. (1990) *Trends Biochem. Sci.* **15**, 53–59.
51. Karlin, A. & Akabas, M. H. (1995) *Neuron* **15**, 1231–1244.